

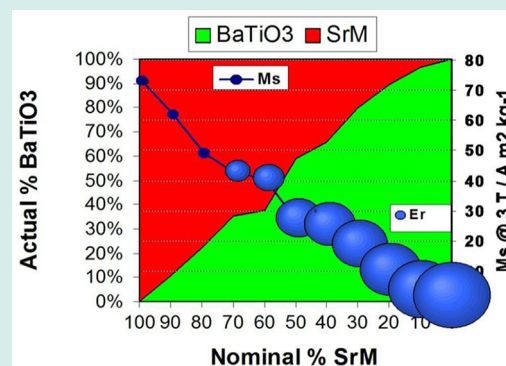
# Combinatorial Bulk Ceramic Magnetolectric Composite Libraries of Strontium Hexaferrite and Barium Titanate

Robert C. Pullar\*

Department Engenharia Cerâmica e do Vidro/CICECO, Universidade de Aveiro, Campus Universitário de Santiago, Aveiro 3810-193, Portugal

**ABSTRACT:** Bulk ceramic combinatorial libraries were produced via a novel, high-throughput (HT) process, in the form of polycrystalline strips with a gradient composition along the length of the library. Step gradient ceramic composite libraries with 10 mol % steps of  $\text{SrFe}_{12}\text{O}_{19}$ – $\text{BaTiO}_3$  (SrM–BT) were made and characterized using HT methods, as a proof of principle of the combinatorial bulk ceramic process, and sintered via HT thermal processing. It was found that the SrM–BT libraries sintered at 1175 °C had the optimum morphology and density. The compositional, electrical and magnetic properties of this library were analyzed, and it was found that the SrM and BT phases did not react and remained discrete. The combinatorial synthesis method produced a relatively linear variation in composition. The magnetization of the library followed the measured compositions very well, as did the low frequency permittivity values of most compositions in the library. However, with high SrM content of  $\geq 80$  mol %, the samples became increasingly conductive, and no reliable dielectric measurements could be made. Such conductivity would also greatly inhibit any ferroelectricity and magnetolectric coupling with these composites with high levels of the SrM hexagonal ferrite.

**KEYWORDS:** bulk ceramic libraries, combinatorial, high-throughput, composite, strontium hexaferrite, barium titanate, magnetolectric



## 1. INTRODUCTION

Combinatorial materials science is the rapid synthesis and analysis of large numbers of compositions in parallel, created through many combinations of a small number of starting materials. Combinatorial searching was initiated in the 1960s for the solid-phase synthesis of peptides by Merrifield,<sup>1</sup> who later won a Nobel Prize for this, but it took until the 1990s for industry to adopt this technique, which is now deemed essential in the pharmaceutical industry, where both sample preparation and analysis are carried out by robots.

The first compositional gradients studied were those naturally occurring in codeposited thin films to construct alloy phase diagrams.<sup>2</sup> In 1970, Hanak proposed his “multiple sample concept” as a way around the traditional, slow, manual, laboratory preparation procedures used to make samples for testing.<sup>3</sup> Robotic search methods for cuprate superconductor thin films were explored by the GEC Hirst Laboratories in the early 1990s,<sup>4</sup> and a series of combinatorial searches in Materials Science were carried out in 1995 by Xiang, Schultz et al.,<sup>5</sup> on a 128 sample combinatorial library of luminescent materials obtained by codeposition of elements on a silicon substrate. Since then the interest in combinatorial materials science and high-throughput (HT) searches has increased greatly, with many review articles<sup>6–9</sup> on this topic. Major companies are investing in its development, and the automation of measurements suitable for combinatorial searches, but such research is still in its infancy.

Most current HT combinatorial research is focused on biotechnology, organic and biological systems, and despite the massive increase in publications on combinatorial or HT methods since 1995, out of over 92 000 combinatorial and HT articles, only 3400 were on Materials Science. Even more startling is that of these, over 2600 articles were on coatings and thin films, mostly on catalysts,<sup>10–12</sup> as well as shape-memory alloys, OLEDs, polymers, organic films and coatings, and only 350 of all combinatorial or HT articles published between 1995 and 2010 were on ceramics or thick films (<0.4%).<sup>13</sup> There is clearly an urgent need to develop non-thin-film-based combinatorial materials science, especially for ceramics, which often have different properties and applications in bulk form compared to their thin film analogues.

Many ceramics have been investigated, and new materials successfully discovered, by searches with combinatorial HT methods.<sup>8</sup> Maybe the best known new material discovered via combinatorial searching is the Co-doped  $\text{TiO}_2$  dilute magnetic semiconductor, leading to an explosion of interest in such materials.<sup>14–16</sup> Other examples include  $\text{Zr}_{0.2}\text{Sn}_{0.2}\text{Ti}_{0.6}\text{O}_2$  dielectrics,<sup>17</sup> high  $\epsilon_r$  microwave dielectrics<sup>18,19</sup> cobalt oxide magneto-resistance materials,<sup>20</sup> energy materials,<sup>9</sup> novel photocatalysts,<sup>21</sup> and catalysts from libraries of thousands of samples.<sup>10</sup> One of

Received: March 18, 2012

Revised: May 15, 2012

Published: June 8, 2012

the most successful fields recently has been phosphors based on rare earths,<sup>22–24</sup> lead free piezoelectrics have been discovered by searching HT films, and of particular interest was a 400 sample Sm- and Sc-substituted BiFeO<sub>3</sub> film library, which showed that only A-site substitutions affected piezoelectric and ferroelectric properties.<sup>9</sup> Of course, virtually all of these ceramics have been discovered as a thin film, or from a solution coated on a catalyst support.

To date, most materials science combinatorial high-throughput methods use thin films: discrete sequentially masked depositions<sup>25</sup> or composition spread codeposition<sup>17,26</sup> by pulsed laser deposition (PLD), liquid source misted chemical deposition (LSMCD),<sup>27</sup> molecular beam epitaxy (MBE)<sup>15</sup> and chemical vapor deposition (CVD),<sup>28</sup> of which PLD is the most common technique. However, often these methods result in uneven film thicknesses and irregular changes in stoichiometry. Combinatorial methods applied to bulk/thick film ceramics usually use either high-throughput synthesis of powders<sup>29</sup> or inkjet printing methods.<sup>30</sup> Much of the work on combinatorial powder synthesis involves just production of a library of powders with a compositional spread, from a process such as hydrothermal synthesis,<sup>31</sup> with no subsequent high-throughput processing. Usually, each sample in the library must be individually prepared (e.g., pressed in a die) from the powder, usually by hand, a rate-limiting, non-HT step. HT automated powder dispersal systems using wells or molds have been developed,<sup>32</sup> but not operating in tandem with a HT combinatorial synthesis process. The inkjet printing process creates a thick film library already laid out on a substrate ready for processing.<sup>33,34</sup> However, in this case, the solution chemistry, stability during a printing run, drying in a regular shape, and reaction with, or lack of adherence to, the substrate, becomes a serious issue, especially in complex multicomponent ceramic systems. The issue of compatibility with substrates is an issue for all inkjet based combinatorial processes, as they need a substrate that can be both printed on and heated during sintering.

The author has used the London University Search Instrument (LUSI) robot to make sintered combinatorial libraries of ceramic compositions by inkjet printing multicomponent mixtures on substrates.<sup>35</sup> LUSI automatically created sintered bulk ceramic libraries by inkjet printing multicomponent mixtures on substrates, then robotically loading and firing the libraries. The bulk ceramics successfully made and characterized as combinatorial libraries were dielectrics, ferroelectrics,<sup>36–38</sup> and ionic conductors,<sup>39</sup> but the inherent rate-limiting problems of the printing process were encountered. It was these experiences that led the author to consider an alternative solution, which gave the benefits of a bulk or thick film ceramic library, but in a much simplified process, and with no overengineering or automation in these first trials.

The novel adapted tape casting process used in this article is a much more simple process. The libraries can be made either on a substrate, or a release tape which can be removed before firing, avoiding substrate problems if necessary. One of the rate limiting steps in combinatorial HT bulk ceramics is the sintering/processing of libraries, as it will be virtually impossible to have all components of different compositions and phases sinter in the same conditions. Parallel multiple-zone firing allows the simultaneous HT firing/sintering of libraries over a range of temperatures or conditions. A unique feature of this process is that it can be used to make combinatorial composite

libraries, such as the ceramic composite libraries reported here, consisting of two ceramics that do not react, but cosinter, to form a ceramic composite library. In this case, the two ceramic components are strontium M-type hexaferrite (SrM, SrFe<sub>12</sub>O<sub>19</sub>), a strongly ferrimagnetic hard ferrite with a large uniaxial magnetic anisotropy,<sup>40</sup> and barium titanate (BT, BaTiO<sub>3</sub>), a well-known ferroelectric and piezoelectric ceramic with a high dielectric permittivity.<sup>37</sup> The author, among others, has previously published work demonstrating that there is no reaction between the similar BaFe<sub>12</sub>O<sub>19</sub> (BaM) ferrite and BT when they are cosintered in composites in ratios of 3:1, 1:1, and 1:3,<sup>41</sup> they maintain individual magnetic and ferroelectric behavior, and that strain-mediated magnetoelectric coupling exists between the two phases of the composite.<sup>42</sup> The property-structure relationships in magnetoelectric (ME) and multiferroic (MF) ceramics are currently poorly understood, particularly for room temperature applications. Combinatorial HT searches appear an ideal way of both generating plentiful data to increase our level of understanding, and discovering novel ME and MF materials with great potential industrial and technological benefits.

As discussed above, most combinatorial materials searches involve thin films. However, many materials are also required in bulk form, and the bulk properties can be quite different to those of thin films, where surface diffusion, strain effects from substrate-lattice mismatch, and surface and skin electrical effects dominate. For example, ferroelectric functions are highly dependent upon strain effects in thin films. Also, most thin films are epitaxial or single crystal, and hence have no grain boundaries, which can have a large effect on electrical, magnetic, dielectric, mechanical and transport properties. From the point of view of constructing large materials properties databases for data mining and prediction of novel compositions, it could be argued that bulk properties are much more relevant than those of thin films. Furthermore, for many applications bulk or thick film ceramics are required. The libraries reported here are in the form of a single polycrystalline strip with a gradient composition in steps, not a layered ceramic. Step gradient ceramic composite libraries with 10 mol % steps of SrM-BT are reported and characterized in this paper, as a proof of principle of the combinatorial bulk ceramic process.

## 2. EXPERIMENTAL SECTION

**2.1. Combinatorial HT Synthesis.** The raw materials used in this work were commercial powders of SrM (Sigma-Aldrich, 99.5%) and BT (Sigma-Aldrich, 99.9%). The bulk ceramic libraries were made through an adapted tape casting process, in which two variable-rate pumps simultaneously fed pastes of SrM and BT powders through a commercial mixer tip, to create a line of mixed paste with a variable composition along its length. The solvent used was xylene, with a weight ratio of 85% ceramic powder to 15% xylene. The two feed pastes, BT and SrM in xylene, were fed to a mixer and then extruded on to the release film via the two syringe pumps. As the rate of one pump is decreased, the rate of the other is increased accordingly, to maintain a continuous overall feed rate (Figure 1a). The nominal changes in composition were 10 mol % steps, resulting in a nine-step library, produced at a constant total feed rate of 1 mL/min. This results in a step gradient library (Figure 1b), produced in around 10 min, with a regular change in composition, collected on a moving bed or belt. It is not doctor bladed as it is extruded, as with a normal tape casting

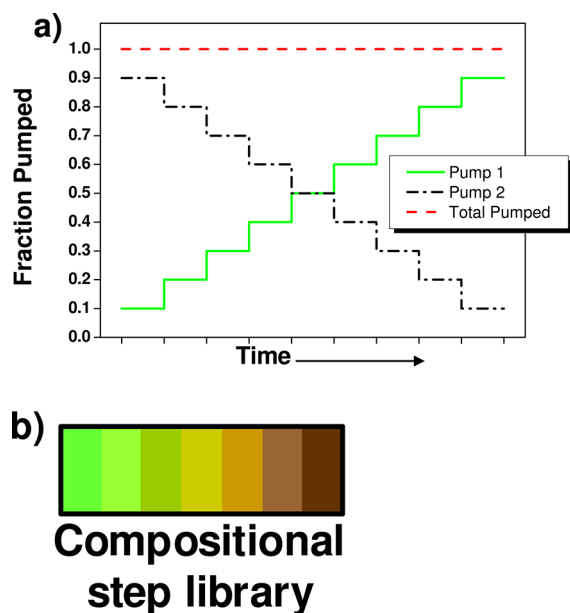


**Figure 1.** Schematic diagrams of (a) the variable fraction–constant total rate pumping process and (b) the step compositional gradient combinatorial libraries produced.

process, but can be either left as a “sausage-like” cylindrical extrusion of several mm diameter and 8 cm length (like toothpaste from a tube), or laterally doctor bladed along its width, to produce a thick film about 1 mm high, 3 cm wide, and 8 cm long. The solvent can then be evaporated to leave a dried green body, tape or thick film. In this case, xylene was evaporated in an oven with circulating air at 60 °C/1 h.

The minimum of solvent is added to the oxides to enable them to be cast (less than in conventional tape casting), as the quality or strength of the tape is not important as long as the compositional gradient is maintained. Unlike a solution-based process, such as ink jet printing, much less volume is lost on drying, leading to reasonably dense ceramics, and no segregation or precipitation effects should occur. The libraries were produced on a plastic release tape attached to a firm, flat support, and once dried they could be carefully slid from this onto a substrate for firing.

The doctor bladed thick film library could be cut lengthways into multiple parallel strips with identical variation in composition. These were then fired in a multiple zone muffle furnace (Figure 2a) with 5 zones, in 25 °C increments in final temperature between each zone, heating at 5 °C/min and with a dwell time of 2 h. Each zone has an independent temperature controller and heating elements, and each has an area of 17 × 11 cm and so can accommodate an entire step library. The libraries were sintered on 120 × 60 × 1 mm alumina sheets. In this case, the libraries were simultaneously heated to 1100, 1125, 1150, 1175, and 1200 °C (Figure 2b). This multiple zone furnace allows parallel HT firing of combinatorial libraries, removing a rate limiting step in the processing of combinatorial ceramics.

**2.2. Characterization of Composite Libraries.** Scanning electron microscope (SEM) micrographs were taken using a Hitachi S-4100 at 10–15 kV. Energy dispersive spectroscopy (EDS) was made using a Rontec UHV Dewar Detektor on the same microscope, on a 40  $\mu\text{m}^2$  area. All of this was carried out on an unpolished and uncoated library. These techniques are both very rapid, and a whole library can be analyzed for

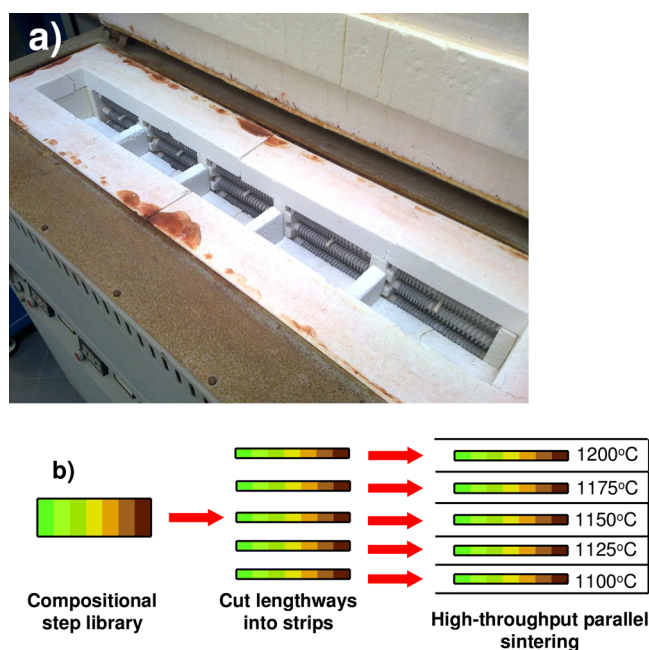


**Figure 2.** (a) Photograph of the five-zone HT furnace. (b) Schematic diagram of the parallel HT thermal processing of combinatorial ceramic libraries.

composition and morphology within 1 h, making this a HT method. X-ray diffraction patterns of the samples were recorded in the region of  $2\theta = 20\text{--}75^\circ$  on a PANalytical X'Pert MRD diffractometer using Cu  $K\alpha$  radiation, with a PANalytical X'celerator Detector, using PANalytical X'Pert software. The X'celerator detector allows the rapid accumulation of data necessary for HT analysis, achieving in <10 min a measurement that would normally take several hours.

The room temperature capacitance and resistivity of the library were measured for each step using a HP 4263B LCR meter cycled between 1 kHz and 1 MHz. Short and open circuit calibrations were carried out to ensure that the measurement errors were <1%. Relative permittivity ( $\epsilon_r$ ) was calculated by the parallel plate capacitor technique, using the equation  $C = (k \epsilon_0 A)/d$ , where  $C$  = capacitance in F,  $d$  = sample thickness in m,  $k$  = relative permittivity ( $\epsilon_r$ ) of the sample,  $A$  = area of the conducting plates in  $\text{m}^2$ , and  $\epsilon_0$  = permittivity of free space ( $8.865 \times 10^{-12} \text{ F m}^{-1}$ ). The errors of this measurement technique have been shown to be very low at low frequencies (<1 MHz) for bulk samples. The electrodes were made by sputtering the library with a thin layer ( $\sim 1 \mu\text{m}$ ) of Ag/Ti. A mask was used with circular holes over the center of each step to give a circular electrode of 5 mm diameter, on the top and bottom of each step. As the library was unpolished, silver conductive paste was also carefully painted on to the electrodes and annealed at 700 °C, to ensure a good contact was made on the rough surface. All steps of the library can be simultaneously measured with multiple contacts, making this a method suitable for HT analysis.

Magnetic measurements were taken on an Oxford Research Instruments vibrating sample magnetometer (VSM) with a helium-cooled 12 T superconducting magnet. The samples were measured in applied fields up to 5 T, at 300 K. At present, such magnetic measurements are not made with a HT technique, and material from each step of the library had to be separated and measured individually in the VSM.



### 3. RESULTS AND DISCUSSION

A nine-step SrM-BT combinatorial library, sintered at 1175 °C/2 h, is shown in Figure 3. This has been laterally doctor bladed

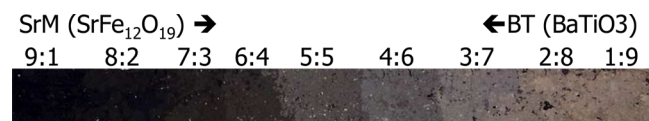


**Figure 3.** Photograph of a nine step SrM-BT combinatorial ceramic composite library (10 mol % steps), sintered at 1175 °C (dimensions  $\sim 80 \times 8 \times 1$  mm).

and cut lengthways into a strip, and it is  $\sim 80 \times 8 \times 1$  mm. The dried libraries are very fragile and inflexible before firing, and must be cut into strips while still moist with solvent. Even after firing, they are too fragile to be cut or polished, and more work needs to be carried out to optimize the combinatorial synthesis process. However, it can clearly be seen that the library consists of nine more-or-less equally sized steps, just from the change in color from the black SrM to the off-white BT. The fragility of the libraries is partly due to their poor densities: this is in part due to inherent initial porosity remaining after the drying process. However, we have also found that trying to cosinter hexagonal ferrites, which sinter at  $\sim 1150$ – $1200$  °C, and BT, which requires up to 1400 °C, is problematic, and the highest densities of  $\sim 90\%$  of maximum theoretical density were achieved at 1250 °C/2 h in 50% BaM–50% BT composites (BaM = BaFe<sub>12</sub>O<sub>19</sub>).<sup>42</sup> SrM ferrites are known to sinter at temperatures around 50 °C lower than BaM,<sup>43</sup> and the optimum sintering temperature for these libraries appeared to be 1175 °C/2 h. Obviously, it was not possible to measure the densities of the individual steps, but the degree of sintering, grain growth, porosity, melting, etc can be assessed from SEM analysis. All subsequent measurements in this paper are of the SrM-BT library sintered at 1175 °C/2 h, except for the pure SrM and BT samples, which were made from the pure powders sintered at 1200 and 1350 °C/2 h, respectively. The library samples are referred to as 9:1 (for a nominal composition of 90 mol % SrM–10 mol % BT), 8:2 (for a nominal composition of 80 mol % SrM–20 mol % BT), etc.

The SEM images of the SrM-BT library, and pure SrM and BT, are shown in Figure 4, all taken at the same magnification, on an unpolished and uncoated library. The pure SrM consists of platy hexagonal grains, all over 1  $\mu\text{m}$  and up to 5  $\mu\text{m}$  in diameter, with some large, clearly hexagonal crystals (Figure 4a). The Pure BT is made up of smaller equiaxed, rounded grains, <1  $\mu\text{m}$  diameter (Figure 4k). Unsurprisingly, the 9:1 composite consists of mostly hexagonal grains (Figure 4b), with a larger proportion of BT grains seen for 8:2 (Figure 4c). At 7:3, the hexagonal SrM grains seem larger and more clearly defined, with increasing amounts of submicrometer BT (Figure 4d), and this becomes even more apparent as the proportion of SrM decreases further, with the hexagonal grains becoming both fewer in number and seemingly larger, up to 5  $\mu\text{m}$  diameter (Figure 4e–f). At 4:6 there are only a few hexagonal grains up to 10  $\mu\text{m}$  diameter dispersed inhomogeneously among the BT grains (Figure 4g), and at 3:7 there are very few hexagonal grains, but definite light and dark areas appear (Figure 4h), with the dark areas containing the remaining hexagonal grains. These differences in contrast are due to charging, with the darker areas being more conductive and draining the surface charge build up from the electron beam, signifying that the ferrite rich areas are more conductive. This high degree of electrical conductivity is a known problem in hexagonal ferrite ceramics, arising from the presence of a small amount of Fe<sup>2+</sup> causing electron hopping between Fe<sup>2+</sup>  $\rightarrow$  Fe<sup>3+</sup>,<sup>44</sup> and as the ferrite rich areas become isolated “islands” in a “sea” of more resistive dielectric BT, this becomes increasingly apparent. Furthermore, in polycrystalline ceramic ferrites, if low resistance grains are separated by highly resistive grain boundaries (in this case, a majority of BT grains), an interfacial polarization can be created that leads to conductivity.<sup>45</sup> This can be reduced in larger grained ferrites, or by doping with other metal 3+ ions that are stable in a 2+ state (e.g., Co<sup>3+</sup>). At 2:8, there are no apparent hexagonal grains, but a small amount of areas in the SEM image show charging (Figure 4i). With the lowest level of SrM, 1:9, the sample had a unique appearance, with scattered dendritic areas of dark, linear grains in a mostly BT ceramics (Figure 4j), their charging suggesting that they were SrM. Similar linear-looking grains have been observed before in hexaferrites among planar hexagonal crystals, and have

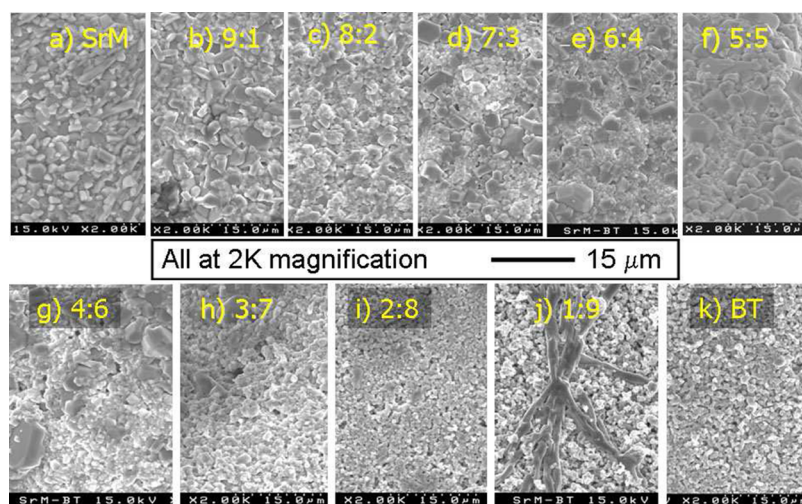


**Figure 4.** SEM images of the nine step (b–j) SrM-BT combinatorial library sintered at 1175 °C. Pure SrM (a) and BT (k) made from noncombinatorial ceramics sintered at 1200 and 1350 °C, respectively.

been shown to be thin hexagonal plates observed edge-on,<sup>46</sup> but no planar or hexagonal crystals were observed in 9:1. This clearly indicates that the samples become progressively less homogeneous on a microscopic scale at low levels of SrM, with the SrM grains clustering together, and this may cause problems for magnetoelectrical applications, as ME coupling will be poor.

EDS analysis was also carried out to ascertain the actual composition of the library steps. First, highly localized EDS measurements on the darker areas seen in Figures 4h–j) showed they were indeed iron and strontium rich, confirming that they contained SrM, and that these elements were absent from the lighter areas, that consisted of BT. Larger area EDS measurements were taken to give a measurement of the nonlocalized compositions, and the results are shown in Figure 5, plotting the actual measured combined atom % of (Fe + Sr)

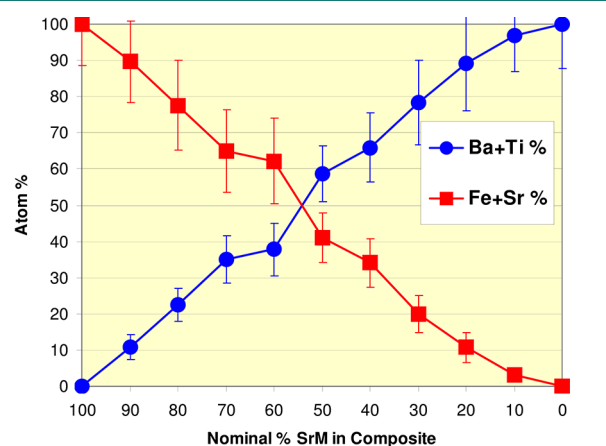


**Figure 5.** EDS analysis of the SrM and BT content in the combinatorial library, against the nominal composition, in mol %.

and (Ba + Ti) against the nominal mol % SrM in each library step. The 100% and 0% measurements were for pure SrM and BT samples. Ideally the two lines should be straight diagonals from corner to corner, but these data show that the composition of the library is reasonably linear. Initially the library seems to be slightly SrM rich up to 6:4, after which the steps begin to contain less SrM than the nominal value. The 5:5 step appears to be closer to 40% SrM/60% BT, and the level of SrM becomes progressively smaller than the nominal levels, as the proportion of BT increases. Nevertheless, as a proof of principle this demonstrates that this combinatorial synthesis process can be used to create bulk ceramic composite libraries, with a reasonably linear variation in composition. The measured values are shown in Table 1.

The XRD patterns of the library are shown in Figure 6a. It can be seen that the two phases have remained discrete, and have not reacted to form any third phases, and the proportions of the two phases follow the nominal compositions well. Expanded views of the region between 30° and 40°, which contains the key peaks for SrM and BT, are shown in Figure 6b and c. The three-dimensional plot gives a better idea of the phase progression through the library, while the stacked 2D layers better show the changes in intensity of the two phases, and the peak positions relative to their known standards (JCPDS 33-1340 and 05-0626). The SrM 100% [114] peak (at 34.19° in standards) varied between 34.28 and 34.42° in the measured patterns, whereas BT 100% [110] peak (at 31.54° in

**Table 1.** Measured Composition, Saturation Magnetization ( $M_s$ ), and Permittivity ( $\epsilon_r$ , at 1 kHz) Values at Room Temperature for the SrM-BT Library

nominal percent SrM	name	BT (mol %)	SrM (mol %)	$M_s$ ( $A\ m^2\ kg^{-1}$ )	$\epsilon_r$ , at 1 kHz
100	SrM	0	100	73.4 <sup>a</sup>	20 <sup>b</sup>
90	9:1	10.36	89.64	62.1	33535
80	8:2	22.45	77.55	49.0	23520
70	7:3	35.07	64.93	42.7	366
60	6:4	37.78	62.22	40.4	521
50	5:5	58.90	41.10	26.6	1063
40	4:6	65.92	34.08	24.5	1399
30	3:7	78.95	20.05	17.8	1665
20	2:8	89.28	10.72	8.8	1952
10	1:9	96.86	3.14	2.1	2401
0	BT	100	0	0	3160 <sup>c</sup>

<sup>a</sup>Literature value.<sup>49</sup> <sup>b</sup>Literature value.<sup>48</sup> <sup>c</sup>Noncombinatorial bulk ceramic BT sample sintered at 1350 °C.

standards) varied between 31.60 and 31.74°, and there was no uniform variation with library composition. These values show that there was no substitution of Ba<sup>2+</sup> by Sr<sup>2+</sup> in BaTiO<sub>3</sub>, as in SrTiO<sub>3</sub> this peak is shifted to 32.45°. The variation in peak position is acceptable for measurements on an unpolished surface, and represents good consistency with the library. No evidence was seen of any reaction with the alumina substrate during firing.

The relative permittivity ( $\epsilon_r$ ) values measured between 1 kHz and 1 MHz at room temperature are shown in Figure 7a), and  $\epsilon_r$  values at 1 kHz are given in table 1. Pure BT has  $\epsilon_r$  of ~3000 at room temperature, and this decreases slightly with increasing frequency, as can be seen for the measured pure BT sample. Hexaferrites are poor dielectrics, with  $\epsilon_r = 10$ –20,<sup>47</sup> and it can be seen that as the proportion of SrM increases, not only did  $\epsilon_r$  of the composite decrease, but it had an increasingly greater effect at higher frequencies. There is a large drop in  $\epsilon_r$  at 6:4 and 7:3, and for 2:8 and 9:1 it increased greatly to tens of thousands. This not a true measure of dielectric polarizability of these two samples, but is indicative of a degree of metal-like conductivity. We were unable to measure the pure SrM sample, but its literature value is used as a marker.<sup>47</sup> The  $\epsilon_r$  values at 1 kHz are shown in Table 1. The resistivity of the library is shown in Figure 7b), and it demonstrates the very large effect that an increasing amount of ferrite has on conductivity. At 2:8 and 1:9, which showed evidence of metal-like conduction in their  $\epsilon_r$  values and a high degree of charging with SEM, the samples had extremely low resistivities, below 10  $\Omega\ m^{-1}$ . All of the steps with higher resistance exhibited a significant decrease in this at higher frequencies, explaining their greater loss of  $\epsilon_r$  at these frequencies. This high degree of electrical conductivity with large proportions of ferrite, and at higher frequencies, will be problematic for many potential ME applications of such materials, and efforts will be made to reduce the conductivity of such ferrite-bearing composites.

SrM single crystals have a reported saturation magnetization ( $M_s$ ) >74  $A\ m^2\ kg^{-1}$ ,<sup>48,49</sup> although lower values are normally seen in sintered polycrystalline ceramics.<sup>43,50,51</sup> The  $M_s$  values at 3 T of the library steps are shown in Figure 8, against nominal composition on the  $x$  axis, and also in Table 1. All steps in the library had virtually fully saturated magnetization at fields of 3 T. In Figure 8, each point is represented by a small pie chart, which shows the actual measured proportion of SrM

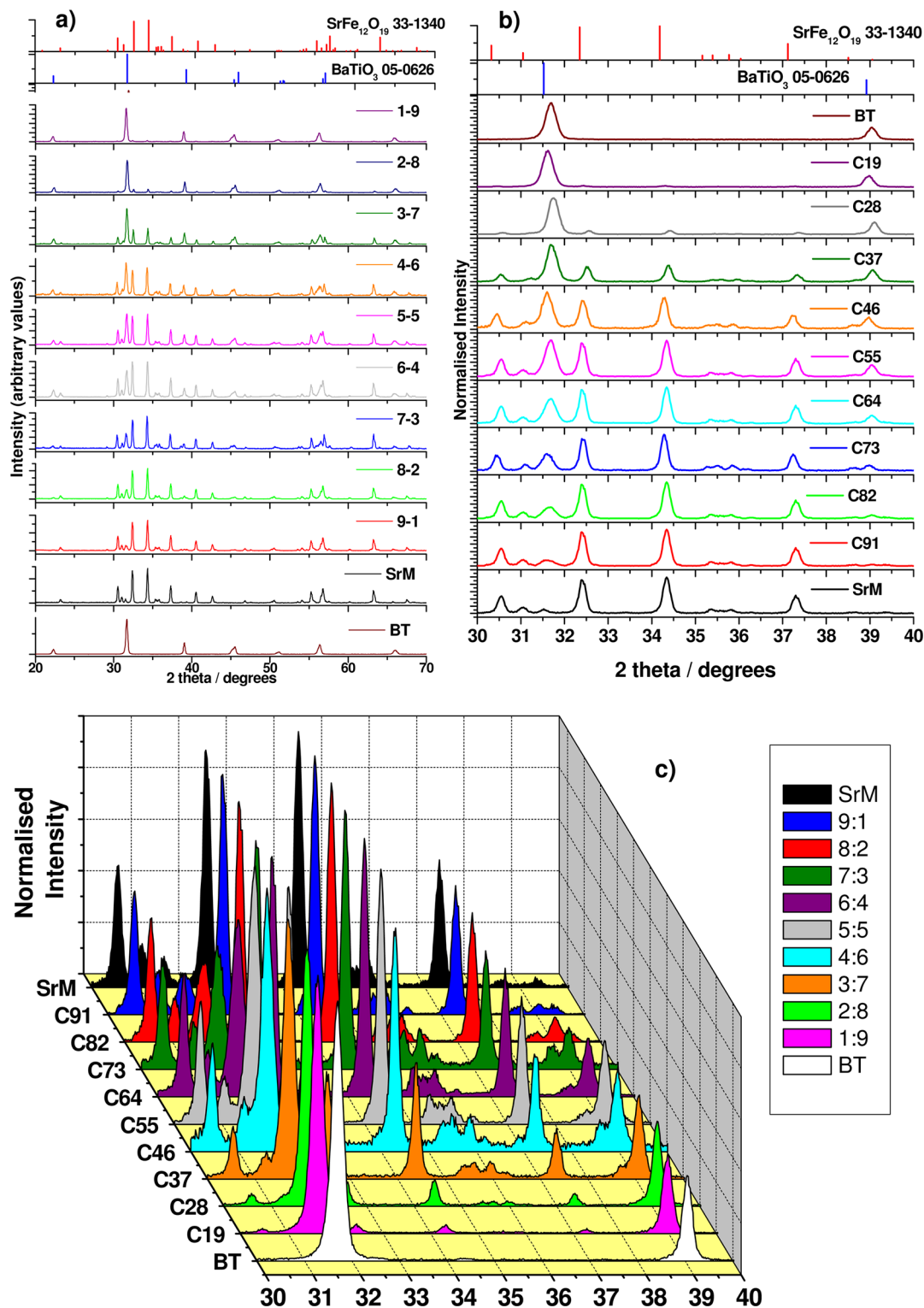


**Figure 6.** (a) XRD spectra of the nine step combinatorial SrM-BT library sintered at 1175 °C. An expanded view of the region between  $2\theta = 30\text{--}40^\circ$  is shown in (b) 2D and (c) 3D. The JCPDS standards 33-1340 (SrM) and 05-0626 (BT) are shown in (a) and (b).

and BT in that step. This may better explain the apparent nonlinearity of the  $M_s$  with composition. It would be expected that this property would be diluted as a function of the proportion of SrM in the composite, and this seems to be the case, but the  $M_s$  values are still as would be expected for quality polycrystalline ceramics. For instance, at 9:1,  $M_s = 62.1 \text{ A m}^2 \text{ kg}^{-1}$  for a sample which is 90% SrM. This equates to a  $M_s$  value

for the SrM itself of  $\sim 69 \text{ A m}^2 \text{ kg}^{-1}$ , a good polycrystalline value, indicating that the magnetic component of the composite library is of high quality. Similarly, for 1:9  $M_s = 2.1 \text{ A m}^2 \text{ kg}^{-1}$  for a sample which is measured as being 3% SrM, equating to  $M_s \approx 67 \text{ A m}^2 \text{ kg}^{-1}$  for the SrM component.

SrM is a hard ferrite, and the coercivity ( $H_c$ ) is usually between  $\sim 300$  and  $450 \text{ kA m}^{-1}$  for polycrystalline SrM



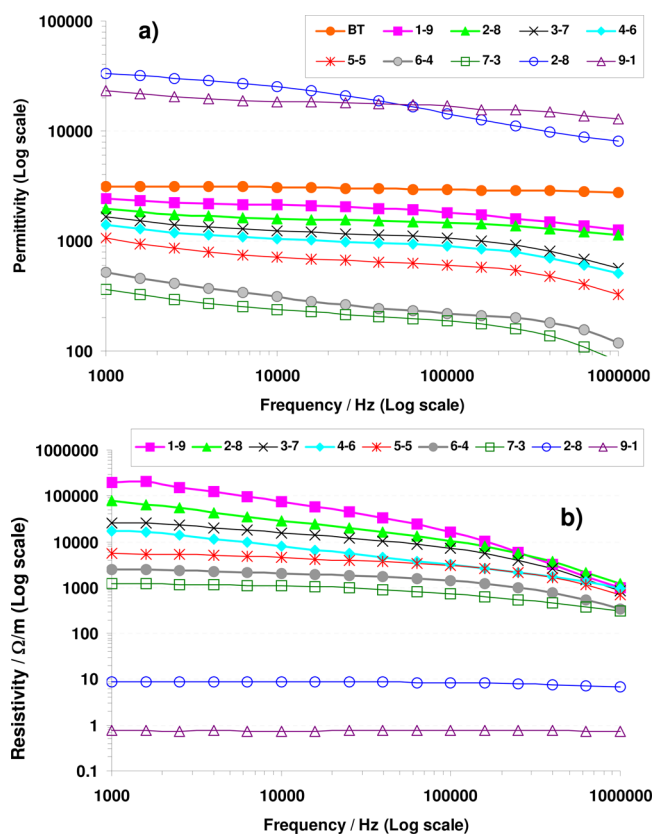


**Figure 7.** Logarithmic plots of (a) permittivity and (b) resistivity of the SrM-BT library sintered at 1175 °C, measured between 1 kHz and 1 MHz at room temperature. The BT sample in a was a noncombinatorial sample sintered at 1350 °C for comparison.

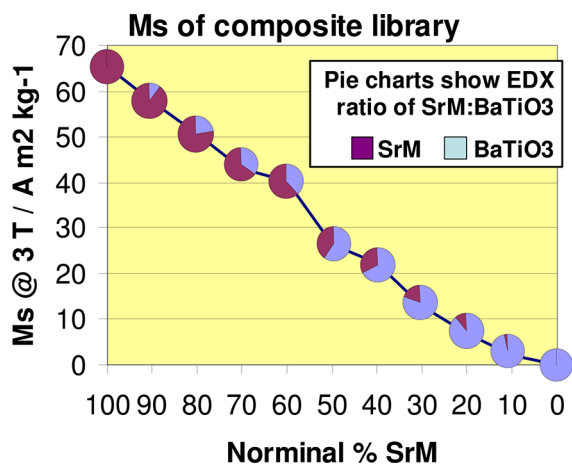


**Figure 8.** Saturation magnetization at 3T vs nominal composition for the SrM-BT library sintered at 1175 °C. The pie chart at each point shows the actual measured proportion of SrM and BT in that step.

ceramics,<sup>48,50</sup> and is highly dependent upon grain size and morphology. However, it was much lower than that expected for a polycrystalline sample with grains in the micrometer range, varying nonlinearly between 140 and 240 kA m<sup>-1</sup> for all steps. The higher values were generally seen in the composites with lower amounts of SrM, but a minimum in  $H_c$  was observed in the 6:4, 5:5 and 4:6 steps. The general trend may be due to SrM grain size increasing with increasing levels of SrM: larger grains contain more domains with Bloch walls, which can move

more easily under an applied field than the reversal of magnetization required in single domain particles. This means that  $H_c$  generally decreases with increasing grain size in SrM. The minimum values may be obtained around the 5:5 composite mixtures because these contained SrM grains with not only large diameters, but they were also thicker, with much greater volumes and hence more magnetic domains. This phenomenon is not yet fully understood, and is currently under further investigation by the author in noncombinatorial ceramic composites.

One of the challenges of combinatorial HT measurements is how to display the many variables analyzed in a visual form that can be easily comprehended. One way of doing this is using glyphs to convey some of the data, as well as just the axes of the plot. Glyphs are graphic data points that convey further information through their form, color, shape, size, etc. Figure 8 is one example of this, in which each point is also a pie chart depicting the measured proportions of the two phases in each step of the library, which is different to the nominal percentage plotted on the  $x$  axis. Another plot using glyphs and colors is shown in Figure 9. In this figure, the  $x$  axis is the nominal

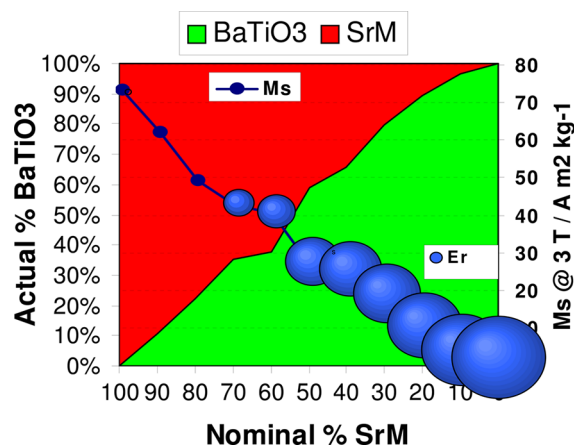


**Figure 9.** Plot of measured composition (black line, left axis), change in phase proportion (red = SrM, green = BT), saturation magnetization ( $M_s$ , blue line and center of points, right axis), and relative permittivity ( $\epsilon_r$ , area of 3D spheres proportional to  $\epsilon_r$ , largest sphere = 3160). The first three points, which are 2D dots, do not represent  $\epsilon_r$  values.

percent SrM in the library step, and the left-hand axis is the measured % of BT, plotted as a line. The actual relative proportions of BT and SrM at any point on that line are shown graphically by the colors pale green and red, respectively, on the background of the plot. This shows clearly the general linear nature of the composition change throughout the library, but also the sudden jump in actual composition around the nominal 6:4 and 5:5 steps, and the SrM deficiency in the BT rich steps. The centers of the blue points represent the  $M_s$  values, showing how they mirror the actual changes in composition very well, with the values displayed on the right-hand axis. The area of the 3D blue spheres represents  $\epsilon_r$ , with the largest sphere at  $x = 0$  being 3160, and the rest decreasing relative to this. In this figure, the  $M_s$  data points for  $x = 100, 90,$  and  $80$  are solid blue 2D dots, to show that these do not represent  $\epsilon_r$  values. This is because the 3D sphere for  $x = 100$  would be too small to see, and the false  $\epsilon_r$  values for  $x = 90$  and  $80$  due to metal-like conduction would be too large for the plot. In this way, this figure represents the nominal composition,

measured composition, relative proportions of the two phases,  $M_s$  values and useful  $\epsilon_r$  values, in a visual manner which can be easily comprehended.

#### 4. CONCLUSIONS

Bulk ceramic combinatorial libraries were produced via a novel, high-throughput (HT), adapted tape casting process, in the form of polycrystalline strips with a gradient composition along the length of the library, not as a layered ceramic. Step gradient ceramic composite libraries with 10 mol % steps of SrM-BT were made and characterized using HT methods, as a proof of principle of the combinatorial bulk ceramic process. They were simultaneously sintered over a range of temperatures in a multiple zone furnace, to enable HT thermal processing and relieve this potential bottleneck in the sintering of ceramic libraries. It was found that the SrM-BT libraries sintered at 1175 °C had the optimum morphology and observed density (from SEM images). The compositional, electrical and magnetic properties of this library were analyzed by HT EDS, XRD and contact capacitance methods, and non-HT VSM. It was found that the SrM and BT phases did not react and remained discrete, and produced reasonably well sintered ceramic composites. The combinatorial synthesis method produced a relatively linear variation in composition, albeit with a jump in composition around the 50–50 mixture, and an increasing degree of SrM deficiency at low SrM content levels. It is not clear why there should be such a difference from the nominal composition for the 50–50 step: the xylene solvent did appear to cause swelling of the syringe gasket, and this may have affected the rate of pumping at some point. Other solvents will be investigated in the future, and the use of all-glass syringes. Due to their fragility, the samples were unpolished, and this will also effect the accuracy of the measurements. The variation in composition was certainly acceptable as a proof of principle for a new combinatorial bulk ceramic synthesis process. The magnetization of the library followed the measured compositions very well, and the low frequency permittivity values of the BT rich samples were good, demonstrating that these composites should have piezoelectric and ferroelectric properties, as well as magnetic. However, with high SrM content of  $\geq 80$  mol %, the samples became increasingly conductive, and no reliable dielectric measurements could be made. Such conductivity would also greatly inhibit any ferroelectricity and magnetoelectric coupling with these composites with high levels of SrM. Further investigations are being made of interesting individual compositions discovered within this combinatorial library. At present the sintered libraries are too fragile to be polished, limiting their ability to be measured by many HT scanning methods such as piezoresponse force microscopy (PFM), magnetic force microscopy (MFM), evanescent microwave probe or scanning evanescent microwave microscope (EMP/SEMM), etc. This matter of improved strength and density needs to be addressed in the future.

#### AUTHOR INFORMATION

##### Corresponding Author

\*E-mail: rpullar@ua.pt.

##### Funding

This work was funded by CICECO and the FCT Ciência 2008 Program.

#### Notes

The authors declare no competing financial interest.

#### REFERENCES

- (1) Merrifield, R. B. Solid-phase peptide synthesis I. The synthesis of a tetrapeptide. *J. Am. Chem. Soc.* **1963**, *85*, 2149–2153.
- (2) Kenedy, K.; Stefansky, T.; Davy, G.; Zacky, V. F.; Parker, E. R. Rapid mapping for determining ternary-alloy phase diagrams. *J. Appl. Phys.* **1965**, *36*, 3808–3810.
- (3) Hanak, J. J. The multiple sample concept in materials research: Synthesis, compositional analysis, and testing of entire multi-component systems. *J. Mater. Sci.* **1970**, *5*, 964–971.
- (4) Hall, S. R.; Harrison, M. T. R. The search for new superconductors. *Chem. Br.* **1994**, *30*, 739–740.
- (5) Xiang, X.-D.; Sun, X.; Briceno, G.; Lou, Y.; Wang, K.-A.; Chang, H.; Wallace-Freedman, W. G.; Chen, S.-W.; Schultz, P. G. A Combinatorial Approach to Materials Discovery. *Science* **1995**, *268*, 1738–1740.
- (6) Koinuma, H.; Tekeuchi, I. Combinatorial solid-state chemistry of inorganic materials. *Nat. Mater.* **2004**, *3*, 429–438.
- (7) Potyrailo, R. A.; Takeuchi, I. Role of high throughput characterization tools in combinatorial materials science. *Meas. Sci. Technol.* **2005**, *16*, 1–4.
- (8) Zhao, J.-C. Combinatorial approaches as effective tools in the study of phase diagrams and composition-structure relationships. *Prog. Mater. Sci.* **2006**, *51*, 557–631.
- (9) Potyrailo, R.; Rajan, K.; Stoewe, K.; Takeuchi, I.; Chisholm, B.; Lam, H. Combinatorial and high-throughput screening of materials libraries: Review of state of the art. *ACS Comb. Sci.* **2011**, *13*, 579–633.
- (10) Farrusseng, D. High-throughput heterogeneous catalysis. *Surf. Sci. Rep.* **2008**, *63*, 487–513.
- (11) Zhang, Y.; McGinn, P. J. Combinatorial screening for methanol oxidation catalysts in alloys of Pt, Cr, Co, and V. *J. Power Sources* **2012**, *206*, 29–36.
- (12) Domènech-Ferrer, R.; Rodríguez-Viejo, J.; Garcia, G. Infrared imaging tool for screening catalyst effect on hydrogen storing thin film libraries. *Catal. Today* **2011**, *159*, 144–149.
- (13) Statistics by the author of this paper, searching on Scopus, in September 2011.
- (14) Matsumoto, Y.; Murakami, M.; Shono, T.; Hasegawa, T.; Fukumura, T.; Kawasaki, M.; Ahmet, P.; Chikyow, T.; Koshihara, S.; Koinuma, H. Room-temperature ferromagnetism in transparent transition metal-doped titanium dioxide. *Science* **2001**, *291*, 854–856.
- (15) Fukumura, T.; Ohtani, M.; Kawasaki, M.; Okimoto, Y.; Kageyama, T.; Koida, T.; Hasegawa, T.; Tokura, Y.; Koinuma, H. Combinatorial search for transparent oxide diluted magnetic semiconductors. *MRS Proc.* **2001**, *700* (S2.6), 10.
- (16) Jin, Z.; Fukumura, T.; Kawasaki, M.; Ando, K.; Saito, H.; Sekiguchi, T.; Yoo, Y. Z.; Murakami, M.; Matsumoto, Y.; Hasegawa, T.; Koinuma, H. High throughput fabrication of transition-metal-doped epitaxial ZnO thin films: A series of oxide-diluted magnetic semiconductors and their properties. *Appl. Phys. Lett.* **2001**, *78*, 3824–3826.
- (17) van Dover, R. B.; Schneemeyer, L. F.; Fleming, R. M. Discovery of a useful thin film dielectric using a combinatorial-spread approach. *Nature* **1998**, *392*, 162–164.
- (18) Green, M. L.; Schenck, P. K.; Chang, K.-S.; Ruglovsky, J.; Vaudin, M. Higher- $\kappa$  dielectrics for advanced silicon microelectronic devices: A combinatorial research study. *Microelectron. Eng.* **2009**, *86*, 1662–1664.
- (19) Chang, H.; Takeuchi, I.; Xiang, X.-D. A low loss composition region identified from a thin film composition spread of  $(\text{Ba}_{1-x}\text{Sr}_x\text{Ca}_y)\text{TiO}_3$ . *Appl. Phys. Lett.* **1999**, *74*, 1165–1167.
- (20) Briceno, G.; Chang, H.; Sun, X.; Schultz, P. G.; Xiang, X.-D. A class of cobalt oxide magnetoresistance materials discovered with combinatorial synthesis. *Science* **1995**, *270*, 273–275.
- (21) Ding, J.; Bao, J.; Sun, S.; Luo, Z.; Gao, C. Combinatorial discovery of visible-light driven photocatalysts based on the  $\text{ABO}_3$ -type



- ((A) Y, La, Nd, Sm, Eu, Gd, Dy, Yb, (B) Al and In)) binary oxides. *J. Comb. Chem.* **2009**, *11*, 523–526.
- (22) Luo, Z.-L.; Geng, B.; Bao, J.; Gao, C. Parallel solution combustion synthesis for combinatorial materials studies. *J. Comb. Chem.* **2005**, *7*, 942–946.
- (23) Chan, T.-S.; Kang, C.-C.; Liu, R.-S.; Chen, L.; Liu, X.-N.; Ding, J.-J.; Bao, J.; Gao, C. Combinatorial study of the optimization of  $Y_2O_3:Bi,Eu$  red phosphors. *J. Comb. Chem.* **2007**, *9*, 343–346.
- (24) Chan, T.-S.; Liu, Y.-M.; Liu, R.-S. Combinatorial search for green and blue phosphors of high thermal stabilities under UV excitation based on the  $K(Sr_{1-x-y})PO_4:Tb^{3+},Eu^{2+}$  system. *J. Comb. Chem.* **2008**, *10*, 847–850.
- (25) Matsumoto, Y.; Murakami, M.; Jin, Z.; Ohtomo, A.; Lippmaa, M.; Kawasaki, M.; Koinuma, H. Combinatorial laser molecular beam epitaxy (MBE) growth of Mg–Zn–O alloy for band gap engineering. *Jpn. J. Appl. Phys.* **1999**, *38*, L603–L605.
- (26) Takahashi, R.; Kubota, H.; Murakami, M.; Yamamoto, Y.; Matsumoto, Y.; Koinuma, H. Design of combinatorial shadow masks for complete ternary-phase diagramming of solid state materials. *J. Comb. Chem.* **2004**, *6*, 50–53.
- (27) Kim, K. W.; Jeon, M. K.; Oh, K. S.; Kim, T. S.; Kim, Y. S.; Woo, S. I. Combinatorial approach for ferroelectric material libraries prepared by liquid source misted chemical deposition method. *Proc. Natl. Acad. Sci. U.S.A.* **2007**, *104*, 1134–1139.
- (28) Kafizas, A.; Hyett, G.; Parkin, I. P. Combinatorial atmospheric pressure chemical vapour deposition (cAPCVD) of a mixed vanadium oxide and vanadium oxynitride thin film. *J. Mater. Chem.* **2009**, *19*, 1399–1408.
- (29) Wendelbo, R. R.; Akporiaye, D. E.; Karlsson, A.; Plassen, M.; Olafsen, A. Combinatorial hydrothermal synthesis and characterisation of perovskites. *J. Eur. Ceram. Soc.* **2006**, *26*, 849–859.
- (30) Evans, J. R. G.; Edirisinghe, M. J.; Coveney, P. V.; Eames, J. Combinatorial searches of inorganic materials using the ink-jet printer: science, philosophy and technology. *J. Eur. Ceram. Soc.* **2001**, *21*, 2291–2299.
- (31) Cabañas, A.; Darr, J. A.; Lester, E.; Poliakov, M. Continuous hydrothermal synthesis of inorganic materials in a near-critical water flow reactor; the one-step synthesis of nano-particulate  $Ce_{1-x}Zr_xO_2$  ( $x = 0-1$ ) solid solutions. *J. Mater. Chem.* **2001**, *11*, 561–568.
- (32) Stegk, T. A.; Janssen, R.; Schneider, G. A. High-throughput synthesis and characterization of bulk ceramics from dry powders. *J. Comb. Chem.* **2008**, *10*, 274–279.
- (33) Zhan, Y.; Chen, L.; Yang, S.; Evans, J. R. G. Thick film ceramic combinatorial libraries: The substrate problem. *QSAR Comb. Sci.* **2007**, *26*, 1036–1045.
- (34) Mohebi, M. M.; Evans, J. R. G. A drop-on-demand ink-jet printer for combinatorial libraries and functionally graded ceramics. *J. Comb. Chem.* **2002**, *4*, 267–274.
- (35) Wang, J.; Evans, J. R. G. London University Search Instrument: A combinatorial robot for high-throughput methods in ceramic science. *J. Comb. Chem.* **2005**, *7*, 665–672.
- (36) Pullar, R. C.; Zhang, Y.; Chen, L.; Yang, S.; Evans, J. R. G.; Alford, N. McN. Manufacture and measurement of combinatorial libraries of dielectric ceramics, Part I: Physical characterisation of  $Ba_{1-x}Sr_xTiO_3$  libraries. *J. Eur. Ceram. Soc.* **2007**, *27*, 3861–3365.
- (37) Pullar, R. C.; Zhang, Y.; Chen, L.; Yang, S.; Evans, J. R. G.; Petrov, P. Kr.; Salak, A. N.; Kiselev, D. A.; Kholkin, A. L.; Ferreira, V. M.; Alford, N. McN. Manufacture and measurement of combinatorial libraries of dielectric ceramics, Part II: Dielectric measurements of  $Ba_{1-x}Sr_xTiO_3$  libraries. *J. Eur. Ceram. Soc.* **2007**, *27*, 4437–4443.
- (38) Pullar, R. C.; Zhang, Y.; Chen, L.; Yang, S.; Evans, J. R. G.; Salak, A. N.; Kiselev, D. A.; Kholkin, A. L.; Ferreira, V. M.; Alford, N. McN. Dielectric measurements on a novel  $Ba_{1-x}Ca_xTiO_3$  (BCT) bulk ceramic combinatorial library. *J. Electroceram.* **2009**, *22*, 245–251.
- (39) Rossiny, J. C. H.; Fearn, S.; Kilner, J. A.; Zhang, Y.; Chen, L. Combinatorial searching for novel mixed conductors. *Solid State Ionics* **2006**, *177*, 1789–1794.
- (40) Pullar, R. C.; Appleton, S. G.; Bhattacharya, A. K. The manufacture, characterisation, and microwave properties of aligned M ferrite fibres. *J. Magn. Magn. Mater.* **1998**, *186*, 326–332.
- (41) Karpinsky, D. V.; Selezneva, E. K.; Bdikin, I. K.; Figueiras, F.; Kamentsev, K. E.; Fetisov, Y. K.; Pullar, R. C.; Krebbs, J.; Alford, N. M.; Kholkin, A. L. Development of novel multiferroic composites based on  $BaTiO_3$  and hexagonal ferrites. *Proc. Mater. Res. Soc.* **2009**, *1161*, 7–12.
- (42) Karpinsky, D. V.; Pullar, R. C.; Fetisov, Y. K.; Kamentsev, K. E.; Kholkin, A. L. Local scale probe of magnetoelectric coupling in  $BaFe_{12}O_{19}$ – $BaTiO_3$  multiferroics. *J. Appl. Phys.* **2010**, *108*, No. 042012.
- (43) Pullar, R. C.; Bhattacharya, A. K. Crystallisation of hexagonal M ferrites from a stoichiometric sol–gel precursor, without formation of the  $\alpha$ - $BaFe_2O_4$  intermediate phase. *Mater. Lett.* **2002**, *57*, 537–542.
- (44) Koops, C. G. On the dispersion of resistivity and dielectric constant of some semiconductors at audiofrequencies. *Phys. Rev.* **1951**, *83*, 121–124.
- (45) Van Uitert, L. G. dc Resistivity in the nickel and nickel zinc ferrite system. *J. Chem. Phys.* **1955**, *23*, 1883–1887.
- (46) Pullar, R. C.; Stacey, M. H.; Taylor, M. D.; Bhattacharya, A. K. Decomposition, shrinkage, and evolution with temperature of aligned hexagonal ferrite fibres. *Acta Mater.* **2001**, *49*, 4241–4250.
- (47) Narang, S. B.; Huidara, L. S. Microwave dielectric properties of M-type barium, calcium, and strontium hexaferrite substituted with Co and Ti. *J. Ceram. Process. Res.* **2006**, *7*, 113–116.
- (48) Kojima, H. *Ferromagnetic Materials*, Vol. 3; Wohlfarth, E. P., Ed.; North-Holland Physics Publishing: Amsterdam, 1982; pp 305–391.
- (49) Shirik, B. T.; Buessem, W. R. Temperature dependence of  $M_s$  and  $K_1$  of  $BaFe_{12}O_{19}$  and  $SrFe_{12}O_{19}$  single crystals. *J. Appl. Phys.* **1969**, *40*, 1294–1296.
- (50) Pullar, R. C.; Bdikin, I. K.; Bhattacharya, A. K. Magnetic properties of randomly oriented BaM, SrM,  $Co_2Y$ ,  $Co_2Z$ , and  $Co_2W$  hexagonal ferrite fibres. *J. Eur. Ceram. Soc.* **2012**, *32*, 905–913.
- (51) Pullar, R. C. Hexagonal ferrites: A review of the synthesis, properties and applications of hexaferrite ceramics. *Prog. Mater. Sci.* **2012**, *57*, 1191–1334.